THE JOURNAL OF BIOLOGICAL CHEMISTRY VOL. 285, NO. 40, pp. 30634–30643, October 1, 2010
© 2010 by The American Society for Biochemistry and Molecular Biology, Inc. Printed in the U.S.A.

Plasma Membrane Ca^{2+}-ATPase Overexpression Depletes Both Mitochondrial and Endoplasmic Reticulum Ca^{2+} Stores and Triggers Apoptosis in Insulin-secreting BRIN-BD11 Cells*[S]

Received for publication, February 22, 2010, and in revised form, July 19, 2010 Published, JBC Papers in Press, July 26, 2010, DOI 10.1074/jbc.M110.116681

Lin Jiang[‡1], Florent Allagnat[§1,2], Evrard Nguidjoe[‡], Adama Kamagate[‡], Nathalie Pachera[‡], Jean-Marie Vanderwinden[¶3], Marisa Brini[‖], Ernesto Carafoli[**], Décio L. Eizirik[§], Alessandra K. Cardozo[§4], and André Herchuelz[‡5]

*From the [‡]Laboratoire de Pharmacodynamie et de Thérapeutique, the [§]Laboratory of Expérimental Medicine, and the [¶]Laboratoire de Neurophysiologie, Université Libre de Bruxelles (ULB), Faculté de Médecine, Bâtiment GE, 808 route de Lennik, B-1070 Brussels, Belgium, the [‖]Department of Biochemistry, University of Padova, 35131 Padova, Italy, and the **Venetian Institute of Molecular Medicine, 35131 Padova, Italy*

Ca^{2+} may trigger apoptosis in β-cells. Hence, the control of intracellular Ca^{2+} may represent a potential approach to prevent β-cell apoptosis in diabetes. Our objective was to investigate the effect and mechanism of action of plasma membrane Ca^{2+}-ATPase (PMCA) overexpression on Ca^{2+}-regulated apoptosis in clonal β-cells. Clonal β-cells (BRIN-BD11) were examined for the effect of PMCA overexpression on cytosolic and mitochondrial [Ca^{2+}] using a combination of aequorins with different Ca^{2+} affinities and on the ER and mitochondrial pathways of apoptosis. β-cell stimulation generated microdomains of high [Ca^{2+}] in the cytosol and subcellular heterogeneities in [Ca^{2+}] among mitochondria. Overexpression of PMCA decreased [Ca^{2+}] in the cytosol, the ER, and the mitochondria and activated the IRE1α-XBP1s but inhibited the PRKR-like ER kinase-eIF2α and the ATF6-BiP pathways of the ER-unfolded protein response. Increased Bax/Bcl-2 expression ratio was observed in PMCA overexpressing β-cells. This was followed by Bax translocation to the mitochondria with subsequent cytochrome *c* release, opening of the permeability transition pore, and apoptosis. In conclusion, clonal β-cell stimulation generates microdomains of high [Ca^{2+}] in the cytosol and subcellular heterogeneities in [Ca^{2+}] among mitochondria. PMCA overexpression depletes intracellular [Ca^{2+}] stores and, despite a decrease in mitochondrial [Ca^{2+}], induces apoptosis through the mitochondrial pathway. These data open the way to new strategies to control cellular Ca^{2+} homeostasis that could decrease β-cell apoptosis in diabetes.

Apoptosis, or programmed cell death, plays a major role in the maintenance of tissue homeostasis. Ca^{2+}, in addition to its contribution to the regulation of cellular processes, may act as a proapoptotic agent, and both intracellular Ca^{2+} depletion or overload may trigger apoptosis (1). Apoptosis can be triggered by three pathways: oligomerization of death receptors, mitochondrial damage, and the ER pathway (2, 3). At the level of the ER, disruption of Ca^{2+} homeostasis causes ER stress with subsequent activation of cysteine protease 12 (caspase-12) that cleaves executioner caspases. The latter cleave structural components of the cell that complete the apoptosis process (1). Before orienting the cell fate to apoptosis, the cell triggers homeostatic mechanisms to preserve ER function, a process known as the unfolded protein response (UPR)[6]. The UPR is mediated by three pathways controlled by transmembrane ER proteins: IRE1α (inositol-requiring transmembrane kinase and endonuclease 1α), PRKR-like ER kinase (PERK), and ATF6 (activation of transcription factor 6). These proteins activate specific transcription factors (such as XBP1s (spliced X- box binding protein 1) and ATF4 (activating transcription factor 4), triggering the expression of UPR-related genes (such as C/EBP homologous protein (CHOP)) (4, 5).

At the level of the mitochondria, a crucial phenomenon leading to cell death is the mitochondrial membrane permeabilization (6). Mitochondrial membrane permeabilization implies the permeabilization of the outer mitochondrial membrane (OMM), the inner mitochondrial membrane or both. In the case of OMM permeabilization, the role of proapoptotic members of the Bcl-2 family (Bax and Bak) appears to be prominent. Upon apoptosis induction, Bax oligomerizes and inserts into the OMM-forming supramolecular openings, allowing the release in the cytoplasm of intermembrane space proteins (including cytochrome *c*) leading to caspase-9 activation. In

* This work has been supported by grants from the Belgian Fund for Scientific Research (Fonds Recherche Scientifique Medicale 3.4593.04 and 3.4527.08), the European Foundation for the Study of Diabetes/Novo Nordisk Programme in Diabetes Research (2005/6), the Juvenile Diabetes Research Foundation International (1-2008-536), the Communauté Française de Belgique (Actions de Recherche Concertées), the European Union (Integrated Project Naimit (FP7) of the European Community), and the Belgium Program on Interuniversity Poles of Attraction initiated by the Belgium State (IUAP P6/40).

[S] The on-line version of this article (available at http://www.jbc.org) contains supplemental "Materials and Methods," Tables S1 and S2, Figs. S1–S6, and additional references.

[1] Both authors contributed equally to this article.

[2] Supported by a fellowship from the "Crédit de Relations Internationales de l'Université Libre de Bruxelles."

[3] Research Director of the Fonds National Recherche Scientifique.

[4] Research Associate of the Fonds National Recherche Scientifique.

[5] To whom correspondence should be addressed: Laboratoire de Pharmacodynamie et de Thérapeutique, Université Libre de Bruxelles, Faculté de Médecine, Route de Lennik, 808, Bâtiment GE, B-1070 Brussels, Belgium. Tel.: 32-2-555-62-01; Fax: 32-2-555-63-70; E-mail: herchu@ulb.ac.be.

[6] The abbreviations used are: UPR, unfolded protein response; PMCA, plasma membrane Ca^{2+}-ATPase; PERK, PRKR-like ER kinase; CHOP, C/EBP homologous protein; OMM, outer mitochondrial membrane; ΔΨ, membrane potential; SERCA, sarco-endoplasmic reticulum Ca^{2+}-ATPase; CPA, cyclopiazonic acid; BiP, immunoglobulin heavy chain binding protein.

contrast, the antiapoptotic members of the Bcl-2 family (*e.g.* Bcl-2 and Bcl-x_L) prevent the oligomerization of Bax and Bak in OMM and pore formation (6). In the case of inner mitochondrial membrane permeabilization, the principal mechanism involved is the so-called "permeability transition," due to the opening of a voltage-dependent channel known as the mitochondrial permeability transition pore (7). The permeability transition pore can be activated by high Ca^{2+} concentrations in the mitochondrial matrix, and a prolonged opening of the permeability transition pore is followed by swelling of the mitochondrial matrix, rupture of the OMM, loss of the membrane potential ($\Delta\Psi$), and the release of cytochrome *c* (8). Due to the low affinity of the mitochondrial Ca^{2+} uptake system (the uniporter), Ca^{2+} is taken up in mitochondria in restricted zones of the cytosol displaying microdomains of high Ca^{2+} concentration, *e.g.* close to the ER Ca^{2+} release channels and/or to the plasma membrane Ca^{2+} channels (9, 10). The different apoptotic pathways may be interrelated. For instance, in the case of sustained release of Ca^{2+} from the ER, the cation may be taken up by mitochondria localized in the Ca^{2+} microdomain, with subsequent mitochondrial membrane permeabilization and cell death (11).

In view of the putative proapoptotic role of Ca^{2+}, the control of intracellular Ca^{2+} may represent a potential approach to prevent or enhance apoptosis and hence to treat diseases characterized by either an increased rate of apoptosis (*e.g.* type 1 diabetes, neurodegenerative disorders, viral infections, etc.) or by a decrease rate of cell death (*e.g.* cancers), respectively. This could be done by overexpressing or down-regulating key mechanisms responsible for Ca^{2+} extrusion from cells, namely the Na/Ca exchanger and the plasma membrane Ca^{2+}-ATPase (PMCA; 12, 13), which have been both implicated in cell death (14–17).

Ca^{2+} plays a major regulatory role in the process of insulin release from the pancreatic β-cell (18), and in type 1 diabetes, the autoimmune destruction of pancreatic β-cells appears to be mediated by apoptosis (19), a phenomenon involving Ca^{2+} (20, 21). In a previous study, we showed that overexpression of Na/Ca exchanger in an insulin-secreting cell line (BRIN-BD11; 22) depleted ER Ca^{2+} stores, leading to ER stress and apoptosis.

In the present study, we examined the impact of PMCA2 overexpression on cell death in BRIN-BD11 cells. To clarify the mechanisms involved in β-cell death, we used the luminescent Ca^{2+} probe aequorin (23) to determine $[Ca^{2+}]$ prevailing in the cytoplasm ($[Ca^{2+}]_i$) and the mitochondria ($[Ca^{2+}]_m$). Furthermore, we examined the expression of several proteins implicated in ER stress response and in mitochondrial membrane permeabilization.

Our data show that stimulation of insulin-secreting cells generates microdomains of high $[Ca^{2+}]_i$ and subcellular heterogeneities in $[Ca^{2+}]_m$ among mitochondria. PMCA2 overexpression depletes cytosolic, ER and mitochondrial Ca^{2+} stores and induces apoptosis via the mitochondrial pathway.

EXPERIMENTAL PROCEDURES

Media, chemicals, and antibodies were purchased from the sources indicated in the supplemental material.

Cell Culture of BRIN-BD11 Cells and Stable Transfection—Cells used in this study were BRIN-BD11 cells obtained by electrofusion of RINm5F with rat islet cells (24). The parental BRIN-BD11 cell line, the two clones overexpressing PMCA2wb, and one clone expressing the vector carrying no insert coding for PMCA2 were characterized previously (25). The PMCA was correctly targeted to the plasma membrane as shown by immunohistochemistry and Western blot, and the clones showed Ca^{2+} responses to K^+-induced membrane depolarization, glucose stimulation, sarco-endoplasmic reticulum Ca^{2+}-ATPase (SERCA) inhibition by thapsigargin, and cyclopiazonic acid (CPA). This and a glucose-induced insulin release comparable with that seen in primary β-cells (25) indicates that this is a good model for primary β-cells. Cells were grown as described previously (24). Control cells (nontransfected and vector-only transfected cells) and clones were stably transfected with wild type (26) or mutated (10) aequorin by the use of Lipofectamine. Positive clones were selected through resistance against Zeocin™ (250 μg/ml, Invitrogen) and verified by RT-PCR. mRNA from Aeq-transfected cells was isolated and reverse transcribed as described previously (25). The primers used in this study are described in supplemental Table S1.

Intracellular Ca^{2+} Concentration Measurements—To reconstitute aequorin, cells expressing wild type aequorin or mutated aequorin were incubated for 2 h at 37 °C with 5 μM of either WT, *n* or *h* coelenterazine in KRB medium at pH 7.4. Cells were placed in the perfusion chamber of a purpose-built thermostatic luminometer (Cairn Research Ltd.) at 22 or 37 °C. The medium used to perfuse the cells was as described previously (25). At the end of each experiment, cells were permeabilized using 100 μM digitonin in medium containing 10 mM Ca^{2+}. This leads to total consumption of aequorin and allows the calibration of the luminescent signal. Luminescence values were transformed into $[Ca^{2+}]$ according to Brini *et al.* (27).

Assessment of Cell Viability, Quantitative RT-PCR, and Western Blot—Cell viability, quantitative RT-PCR, and Western blot were performed as described in the supplemental "Materials and Methods."

Mitochondria Morphology, Activity, and $\Delta\Psi m$ Measurement—Mitochondrial morphology was evaluated using MitoTracker® Green. Cells were incubated with the probe (100 nM) during 30 min at 37 °C and examined using fluorescence microscopy. Mitochondrial activity was determined by the 3-(4,5-dimethylthiazol-2-yl)-2,5-diphenyl tetrazolium bromide assay as described previously (22).

$\Delta\Psi m$ was determined using the fluorescent probe DePsipher™, a green monomeric compound (510/527 nm), which aggregates in the mitochondria upon membrane polarization, forming an orange-red fluorescent compound (585/590 nm; 28). Cells were trypsinized, incubated in the presence of DePsipher, washed, and processed by flow cytometry. Photomultiplier settings were adjusted to detect green monomers and red aggregates fluorescence on the FL1 (530 nm) and FL2 (585 nm) detectors, respectively.

Cytochrome c Release and Bax Translocation—Cells were fixed in fresh 4% paraformaldehyde, rinsed in PBS, permeabilized for 10 min in PBS-Triton X-100 0.1%. Slides were then incubated overnight at 4 °C in the presence of polyclonal rabbit

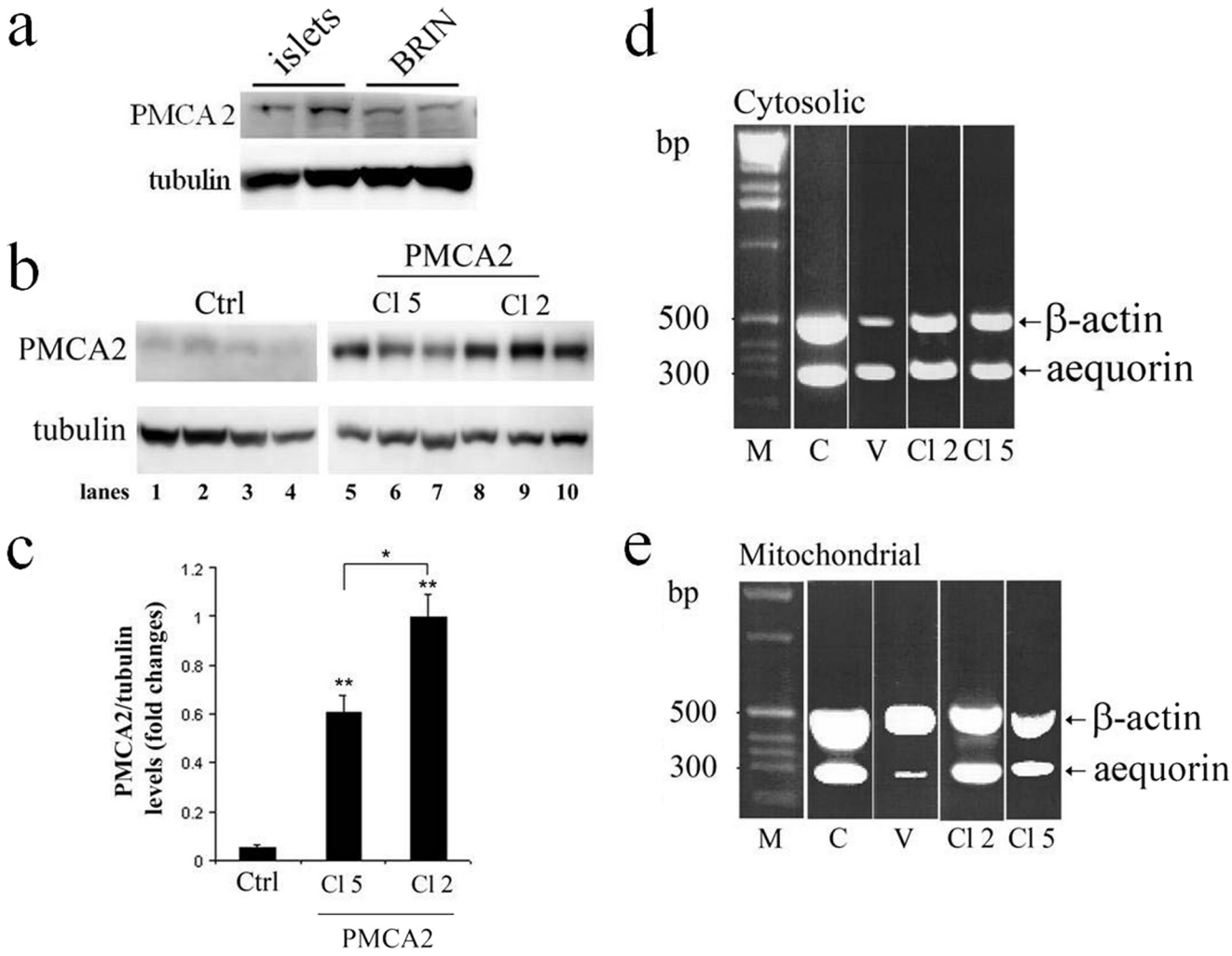

FIGURE 1. **Western blot analysis of PMCA2 in rat islets and in PMCA2-transfected and nontransfected BRIN-BD11 cells and aequorin transfection.** *a* and *b*, Western blot analyses of PMCA in rat islet cells and control BRIN-BD11 cells (*a*) and in nontransfected (control; *Ctrl*) and PMCA2-transfected BRIN-BD11 cells (*b*) using an antibody directed against PMCA2 reveal the presence of the endogenous PMCA2 (*b*, *lanes 1–4*) and the PMCA2-transfected clone 5 (*b*, *Cl 5*, lanes 5–7) or clone 2 (b, *Cl 2*, *lanes 8–10*). *c*, quantitative assessment of PMCA2 levels normalized to the tubulin levels in three independent experiments revealed that PMCA2 expression was significantly higher in clone 2 as compared with clone 5. Results are means of three independent experiments. **, $p < 0.01$ *versus* nontransfected control. *d* and *e*, RT-PCR amplification yielded two bands of 298 bp for aequorin and 589 bp for β-actin (*c*, cytosolic; *d*, mitochondrial). 1 kb DNA ladder molecular weight marker (*M*, sizes in bases). *C*, control cells (nontransfected); *V*, vector-transfected cells); *Cl 2* and *Cl 5*, BRIN-BD11 cells transfected with PMCA2 (clones 2 and 5, respectively). The PCR products were separated by agarose gel electrophoresis and stained with ethidium bromide.

anti-Bax (1/1000) and monoclonal mouse anti-cytochrome *c* (1/1000) and anti-ATP synthase-β (1/1000). Cells were washed and further exposed for 1 h to anti-mouse Alexa Fluor 546 and anti-rabbit Alexa Fluor 488-conjugated antibodies (1/1000). After washing, cells stained with Hoechst were mounted and photographed using fluorescence microscopy. A minimum of 400 cells was counted in each experimental condition by two independent observers, one of them unaware of sample identity.

Statistical Analysis—Data are presented as means ± S.E. Comparisons were performed using Student's *t* test or analysis of variance with post test with Bonferroni correction.

RESULTS

Expression of Aequorin and PMCA2—PMCA2 protein expression as determined by Western blot analysis showed a clear band at the expected molecular range (~135 kDa) that was similar in BRIN-BD11 cells and in rat islet cells (Fig. 1*a*). PMCA2-overexpressing cells (clones 2 and 5) showed a markedly increased amount of the 135-kDa protein ($p < 0.01$; Fig. 1*b*). Densitometric analyses of Western blots further demonstrated that clone 2 expressed significantly higher levels of PMCA2 than clone 5 (Fig. 1*c*).

Quantitative PCR analysis yielded two bands of 298 bp for aequorin and of 589 bp for β-actin, respectively, for cytosolic (Fig. 1*d*) and mitochondrial aequorin transfected cells (Fig. 1*e*). The level of aequorin expression was similar in all preparations, except for mitochondrial aequorin in vector-transfected cells where it was lower.

Measurement of [Ca^{2+}] in Cytosol and Mitochondria—Aequorin was used to measure [Ca^{2+}] in the cytosol ([$Ca^{2+}]_i$) and the mitochondria ([$Ca^{2+}]_m$) of BRIN cells. Fig. 2*a* shows the effect of 5 short (30 s) stimulations with K^+ (50 mM) on [$Ca^{2+}]_i$ in cells stably expressing cytosolic aequorin, reconstituted with WT coelenterazine and carried out at 22 °C. The stimulations

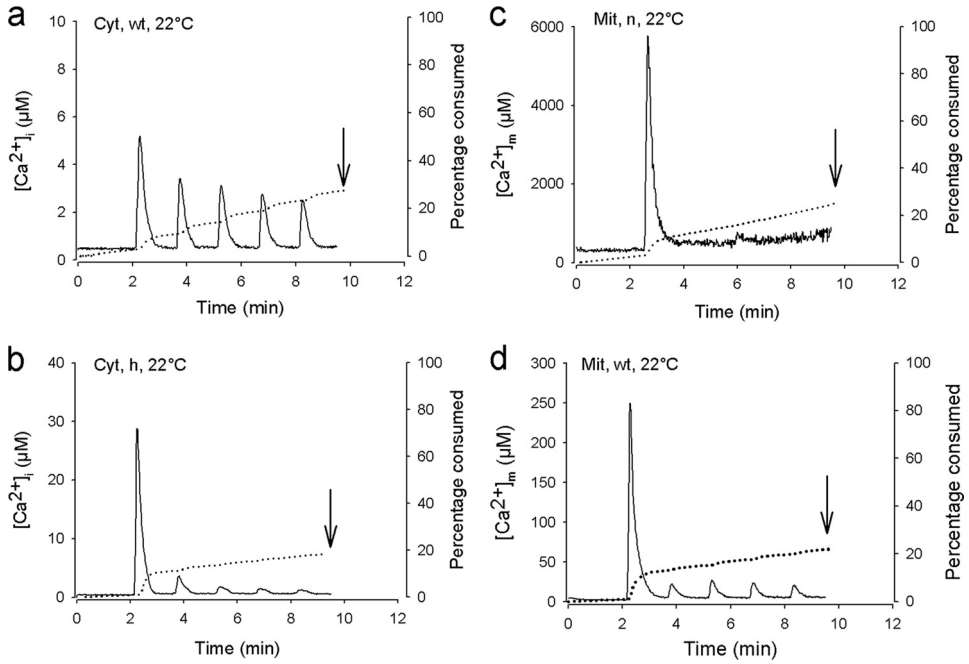

FIGURE 2. **Effect of KCl (50 mM) on $[Ca^{2+}]_i$ and $[Ca^{2+}]_m$ in control BRIN-BD11 cells.** *a* and *b*, effect of five successive exposures (30 s) to KCl on $[Ca^{2+}]_i$ (*solid line*) and aequorin consumption (*dotted line*) using wild type aequorin (*Cyt-Aeq*) recombined with wild type coelenterazine (*WT*) and coelenterazine h (*h*) at 22 °C. The first $[Ca^{2+}]_i$ peak value averaged 5.51 ± 0.45 μM (*a*). *c* and *d*, effect of five successive exposures (30 s) to KCl on $[Ca^{2+}]_m$ (*solid line*) and aequorin consumption (*dotted line*) using mutated aequorin (*Mit*) recombined with coelenterazine *n* (*c*) or WT coelenterazine (*d*, WT) at 22 °C. The value reached during the first peak averaged 5062 ± 990 μM and 162 ± 16 μM, respectively. The total amount of aequorin consumption was measured at the end of each experiment by exposing the cells to 100 μM digitonin in 10 mM Ca^{2+} to permeabilize the plasma membrane to fully expose cellular aequorin to Ca^{2+} and totally consume it to calibrate the luminescent signal. The *dotted line* illustrates the progressive consumption of the dye due to Ca^{2+} exposure. The curves shown are representative of eight individual experiments in each panel, except *b* and *d*, where $n = 12$ and 16, respectively.

were followed by exposure of the cells to digitonin to permeabilize the plasma membrane to calibrate the luminescent signal (data not shown) (23). K^+ induced five consecutive increases in $[Ca^{2+}]_i$ with a progressive but limited reduction of the signal with time, indicating limited consumption of the dye (*dotted line*). A similar phenomenon was observed at 37 °C, except that the value of the peaks were slightly lower (supplemental Fig. S1*a*). The limited consumption of aequorin indicates that the affinity of the complex is adequate and that the increase in $[Ca^{2+}]_i$ measured in response to K^+ represents the exact change in $[Ca^{2+}]_i$ induced by the stimulus. The recombination of aequorin with a more sensitive coelenterazine (*h*) led to a more important consumption of the dye during the first exposure to K^+ during which a $[Ca^{2+}]_i$ of 35 μM was reached. (Fig. 2*b*). The consumption of aequorin also enables it to be used in detecting subcellular heterogeneities in $[Ca^{2+}]$ (10). Indeed, after aequorin consumption in areas of high $[Ca^{2+}]$, the measurements reflect only the behavior of low $[Ca^{2+}]$ areas. This indicates that $[Ca^{2+}]$ up to 35 μM are reached in limited zones of the cytoplasm during cell stimulation. In agreement with this, a concentration of ~7.37 ± 1.28 μM was reached during the second peak, reflecting the rise of $[Ca^{2+}]$ in low $[Ca^{2+}]$ areas, a value comparable ($p > 0.1$) with that measured using WT coelenterazine (Fig. 2*a*). When aequorin was recombined with a low affinity coelenterazine (*n*), very small signals were observed (data not shown), indicating that the affinity of the complex was too low to measure $[Ca^{2+}]_i$.

To measure $[Ca^{2+}]_m$, the low affinity aequorin targeted to the mitochondria was used and recombined with either *n* or WT coelenterazine and carried out at 22 °C. In both cases, when the cells were exposed to five short K^+ stimulations, a major initial increase in $[Ca^{2+}]_i$ was observed (Fig. 2, *c* and *d*). For the experiment carried out with coelenterazine *n*, no further increases in $[Ca^{2+}]_i$ were observed on further K^+ stimulation, whereas small increases were observed when WT coelenterazine was used. This indicates subcellular heterogeneities in $[Ca^{2+}]_m$ among mitochondria. Thus, during the first K^+ stimulation, some mitochondria show large (mM range) increases in $[Ca^{2+}]_m$ with complete consumption of aequorin. Subsequent stimulations only evoke smaller responses (μM range) from other mitochondria.

Effect of PMCA2 Overexpression on $[Ca^{2+}]_i$ and $[Ca^{2+}]_m$—Supplemental Fig. S1*b* shows that $[Ca^{2+}]_i$ data similar to that obtained in nontransfected cells (Fig. 2*a*) were obtained in vector-transfected cells for wild type aequorin at 22 °C. The first peak $[Ca^{2+}]_i$ value averaged 5.64 ± 0.39 μM at 22 °C, a value similar to that observed in nontransfected cells (Fig. 2*a*, $p > 0.8$). In clone 2 of PMCA2-transfected cells, the K^+-induced increases in $[Ca^{2+}]_i$ were reduced by ~65% (Fig. 3*a*) compared with control cells. In clone 5 (Fig. 3*b*), the increases were reduced by 45%. A similar picture was observed at 37 °C (data not shown, $p < 0.001$).

Similar to $[Ca^{2+}]_i$, supplemental Fig. S1*c* shows that the data for $[Ca^{2+}]_m$ obtained in vector-transfected cells at 22 °C were in a similar range to those obtained in nontransfected cells (Fig. 2*c*). Compared with control cells, PMCA2-transfected cells (Fig. 3, *c* and *d*) showed a 82 and 70% decrease in a K^+-induced rise in $[Ca^{2+}]_m$ in clones 2 and 5, respectively ($p < 0.001$). Similar data were obtained at 37 °C (data not shown).

To examine the effect of glucose on $[Ca^{2+}]_i$ and $[Ca^{2+}]_m$, the experiments were carried out at 37 °C, and the exposure to 11.1 mM of the sugar was continuous from min 2 (supplemental Fig. S2). Glucose (11.1 mM) induced in most cases a succession of brief spikes of $[Ca^{2+}]_i$ on a flat basal level in control (supplemental Fig. S2*a*) or vector-transfected cells (supplemental Fig. S3*a*). In some cases, there was a modest or more important increase in basal level (supplemental Fig. S3, *b* and *c*). A quite similar picture is seen in single (dispersed) β-cells (29) and BRIN-BD11 cells using fura-2 to measure $[Ca^{2+}]_i$ (25). In PMCA2-overexpressing cells, the spikes were reduced in number and size (supplemental Fig. S2, *c*, and *d*, Fig. S2, *c* and *e*), and there were no increases in basal level. The value of the highest spike was 2.30 ±

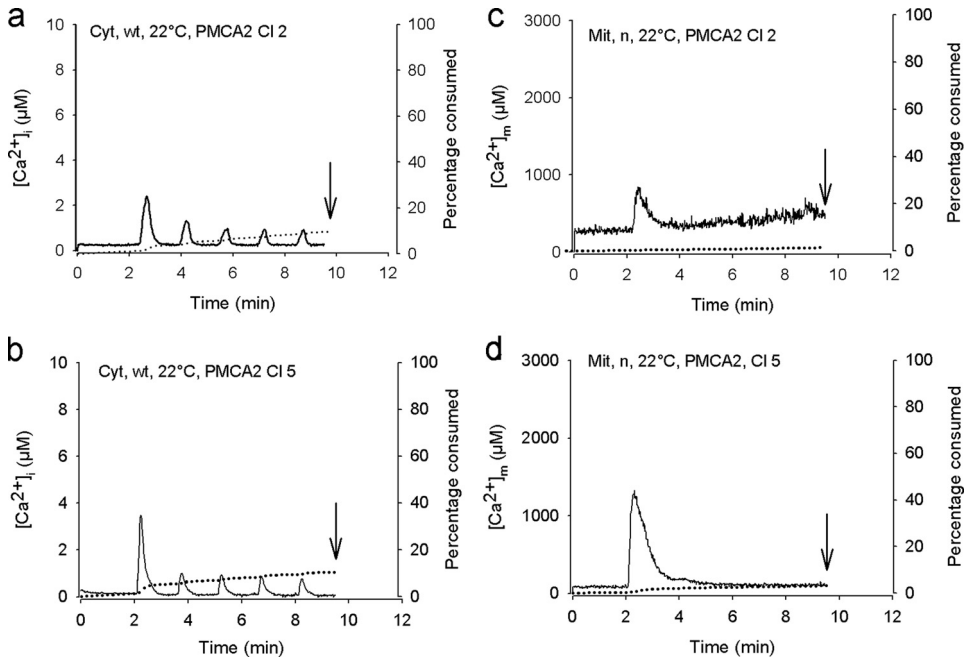

FIGURE 3. **Effect of PMCA2 overexpression on 50 mM KCl-induced increase in $[Ca^{2+}]_i$ and $[Ca^{2+}]_m$.** *a* and *b*, effect of five successive exposures (30 s) to KCl on $[Ca^{2+}]_i$ using wild type aequorin (*Cyt*) recombined with wild type coelenterazine (*WT*) at 22 °C in PMCA2-overexpressing cells (*a*, clone 2, first peak value, 2.63 ± 0.56 μM; *b*, clone 5, first peak value, 3.95 ± 0.69 μM). *c* and *d*, effect of five successive exposures (30 s) to KCl on $[Ca^{2+}]_m$ using mutated aequorin (*Mit*) recombined with coelenterazine n (*n*) at 22 °C in PMCA2-overexpressing cells (*c*, clone 2; *d*, clone 5). Shown is the same presentation as in Fig. 2. The curves shown are representative of eight individual experiments in each case.

0.20 μM in control and 1.30 ± 0.17 μM and 1.52 ± 0.20 μM in PMCA2-overexpressing cells, clones 2 and 5, respectively ($p < 0.05$). Likewise, the number of spikes measured in control cells averaged 4.54 ± 0.62 for the whole period of exposure to glucose, and 1.89 ± 0.31 and 2.13 ± 0.23 in PMCA2-overexpressing cells, clones 2 and 5, respectively ($p < 0.001$).

With respect to $[Ca^{2+}]_m$, spikes also were observed in response to glucose, but compared with $[Ca^{2+}]_i$, their number was low and no elevation in the baseline value was observed (supplemental Fig. S2*b*). Again, in PMCA2-overexpressing cells, the spikes were reduced in number and size (supplemental Fig. S2, *d* and *f*). In clone 2 of PMCA2-overexpressing cells, there were no spikes in 8 of 12 experiments (supplemental Fig. S2*d*).

Altogether, our data show that insulin-secreting cell stimulation generates microdomains of high $[Ca^{2+}]_i$ and subcellular heterogeneities in $[Ca^{2+}]_m$ among mito-

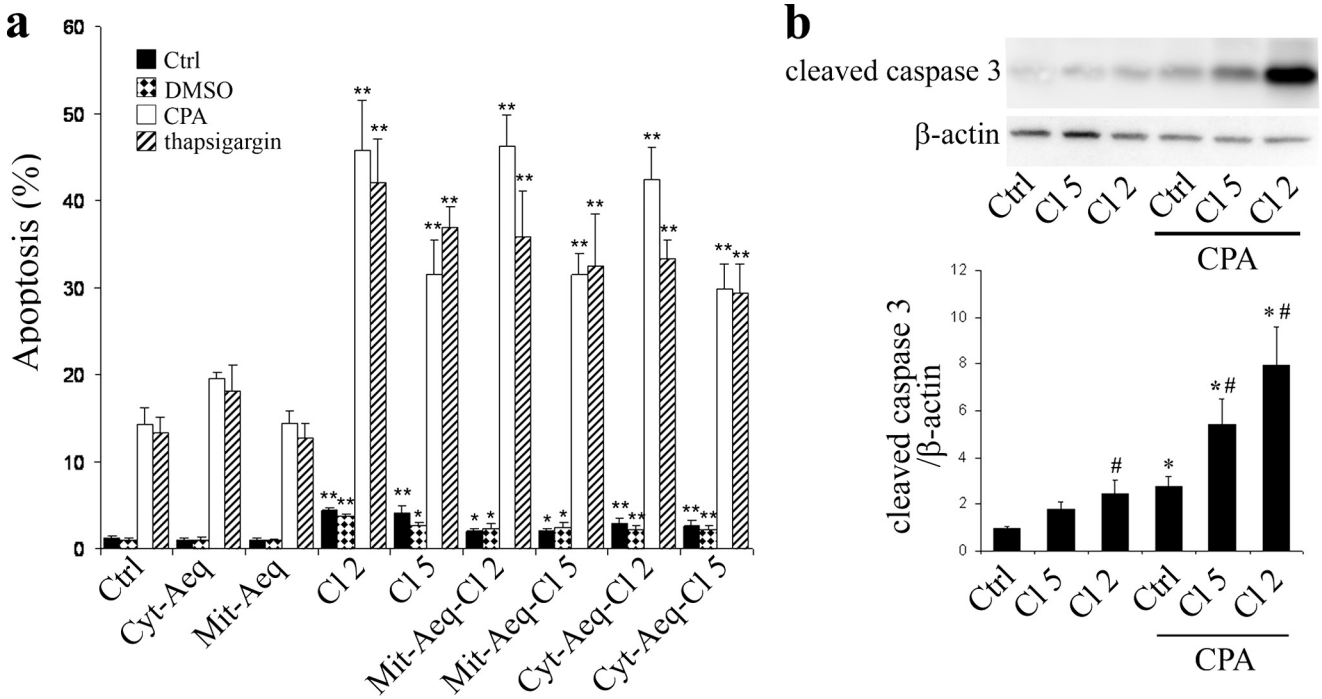

FIGURE 4. **Effect of PMCA2 overexpression on cells viability and caspase-3 cleavage.** *a*, cell viability. Nontransfected BRIN BD-11 cells (*Ctrl*) or different clones of BRIN cells transfected with PMCA2, clone 2 (*Cl 2*), or clone 5 (*Cl 5*) and/or aequorin targeted to the cytosol (*Cyt-Aeq*) or the mitochondria (mutated aequorin (*Mit-Aeq*)) were untreated (*black bars*) or treated for 24 h with CPA (*white bars*), thapsigargin (*striped bars*), or the solvent DMSO (*dotted bars*). Apoptosis levels were evaluated by observation under a microscope after Hoechst 33342-propidium iodide staining. The data are expressed as the percentage of apoptotic cells over the total number of cells counted ± S.E. Results are means of three to five independent experiments. *, $p < 0.05$ and **, $p < 0.01$ *versus* respective nontransfected control. *b*, caspase-3 cleavage. Western blot analyses of nontransfected (*Ctrl*) and PMCA2-transfected cells, clone 2 (*Cl 2*) or clone 5 (*Cl 5*) using an antibody directed against the cleaved caspase-3 fragment. *Upper panel*, representative blot of caspase-3 and β-actin expression. *Lower panel*, quantitative assessment of cleaved caspase-3 levels normalized to the β-actin levels. Results are means of five independent experiments. *, $p < 0.05$ *versus* respective nontreated control. #, $p < 0.05$ *versus* respective nontransfected condition.

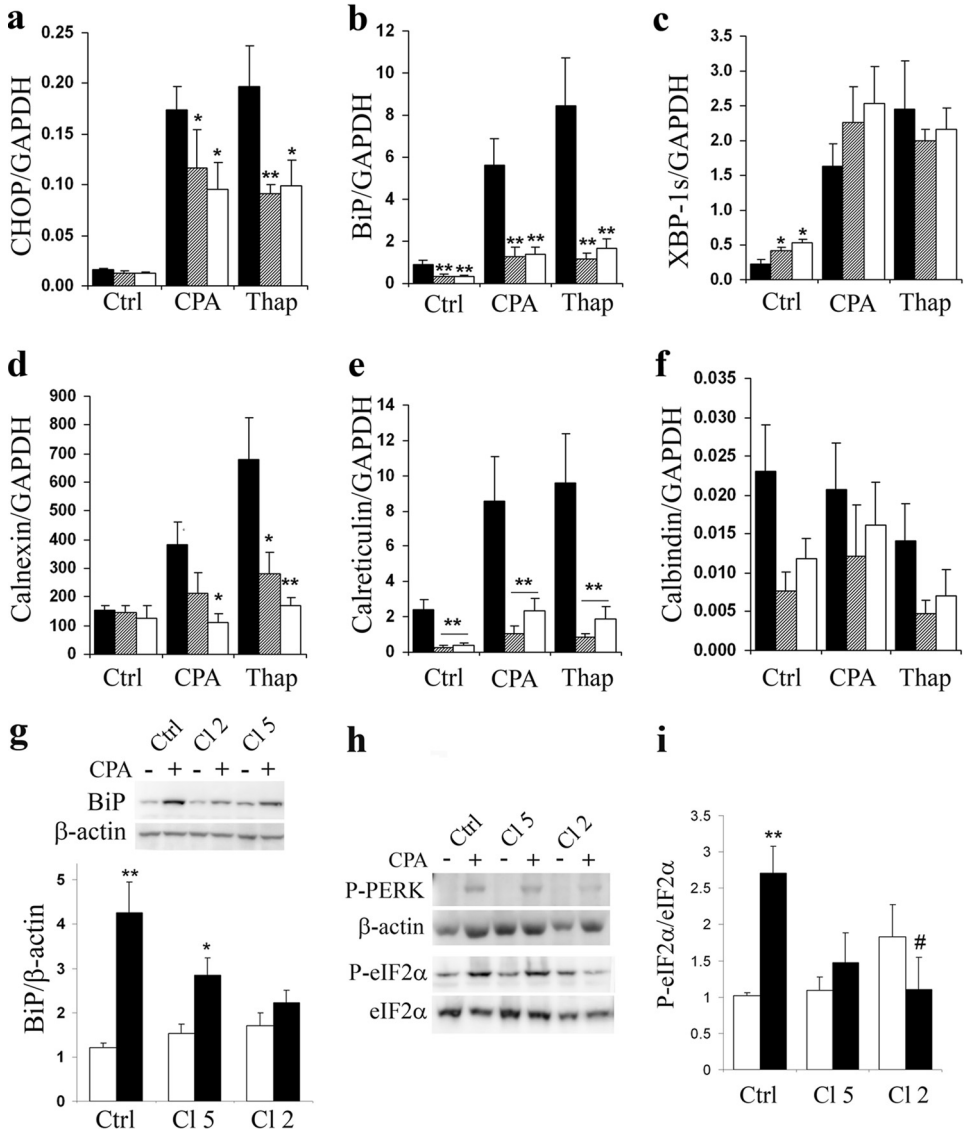

FIGURE 5. **Effect of PMCA2 overexpression on ER-related genes and on the BiP and PERK-eIF2α pathway of the UPR.** *a–f*, ER-related genes. Control cells (*black bars*) or cells stably transfected with PMCA2, clone 5 (*striped bars*), and clone 2 (*white bars*) were treated or not for 24 h with CPA (50 μM) or thapsigargin (*Thap*; 100 nM). mRNAs were extracted, and real-time PCR experiments were performed. Data represent expression of CHOP (*a*), BiP (*b*), XBP1s (*c*), calnexin (*d*), calreticulin (*e*), and calbindin (*f*) normalized per GAPDH expression. Results are means ± S.E. of four independent experiments. *, $p < 0.05$ and **, $p < 0.01$ *versus* respective nontransfected condition. *g*, BiP. Control cells or cells stably transfected with PMCA2, clone 5 (*Cl 5*), and clone 2 (*Cl 2*) were treated (*black bars*) or not (*white bars*) for 24 h with CPA (50 μM). *Upper panel*, representative Western blot of BiP expression. *Lower panel*, quantitative assessment of BiP protein expression normalized to the β-actin levels. Results are means ± S.E. of four independent experiments. *, $p < 0.05$; **, $p < 0.01$. *h* and *i*, PERK-eIF2α pathway. *h*, representative Western blot of PERK and eIF2α phosphorylation. *i*, quantitative assessment of eIF2α phosphorylation, normalized to total eIF2α levels. Results are means ± S.E. of four independent experiments. **, $p < 0.01$ *versus* nontreated condition; #, $p < 0.05$ *versus* CPA-treated nontransfected BRIN-BD11 cells.

chondria and that PMCA2 overexpression depletes cytosolic and mitochondrial Ca^{2+} stores. We then examined the effect of PMCA2 on cell viability.

Effect of PMCA2 Overexpression on Cell Viability—PMCA2-overexpressing clones displayed an increased rate of basal apoptosis (Fig. 4*a*). The SERCA inhibitors CPA (50 μM) and thapsigargin (500 nM) increased apoptosis levels in all clones, but this was more marked in PMCA2-overexpressing cells (Fig. 4*a*). The rate of apoptosis induced by CPA was significantly higher in clone 2 than in clone 5, in line with the higher expression of PMCA2 in clone 2 (Fig. 1, *b* and *c*). PMCA2-overexpressing cells also displayed increased levels of caspase-3 cleavage compared with control cells, in the absence or presence of CPA (Fig. 4*b*). Under these conditions, the rate of caspase-3 cleavage tended to be higher in clone 2 than in clone 5.

Mechanism of Apoptosis—We then examined whether PMCA2 overexpression induced apoptosis through the ER or mitochondrial pathway. We first examined the expression of several genes and proteins implicated in the UPR. Under basal conditions, PMCA2 overexpression did not affect CHOP expression (Fig. 5*a*), decreased BiP expression (Fig. 5*b*), and increased XBP1s expression (Fig. 5*c*). A 24-h CPA or thapsigargin treatment resulted in a significant increase in CHOP, BiP, and XBP1s expression in all cells (Fig. 5, *a–c*). The latter increase in CHOP and BiP expression was reduced by ~30 and 50% in PMCA2-overexpressing cells (both clones), whereas that of XBP1s showed no difference compared with control cells. The expression of the ER Ca^{2+} chaperone calreticulin was strongly impaired under both basal and treated conditions (Fig. 5*e*), whereas calnexin expression, which was significantly increased in response to CPA and thapsigargin in control cells, was less affected by the SERCA inhibitors in PMCA2-overexpressing cells (Fig. 5*d*). The expression of the cytosolic Ca^{2+}-binding protein calbindin was not significantly modified in PMCA2-overexpressing cells, but there was a trend for lower values than in control cells (Fig. 5*f*). At the protein level, there was no decrease in basal BiP expression, but the increase in expression induced by CPA was partially lost in clone 5 and fully suppressed in the clone 2 of PMCA2-overexpressing cells (Fig. 5*g*). The decreased CHOP mRNA response to SERCA inhibitors in PMCA-overexpressing cells suggested a decreased PERK-eIF2α pathway activity, and, indeed, we observed that both PERK and eIF2α phosphorylation were decreased in PMCA2-overexpressing cells when exposed to CPA (Fig. 5, *h* and *i*). PMCA2 overexpression failed to increase caspase-12 expression under basal condition and to affect its expression activated by CPA or thapsigargin (supplemental Fig. S4*a*).

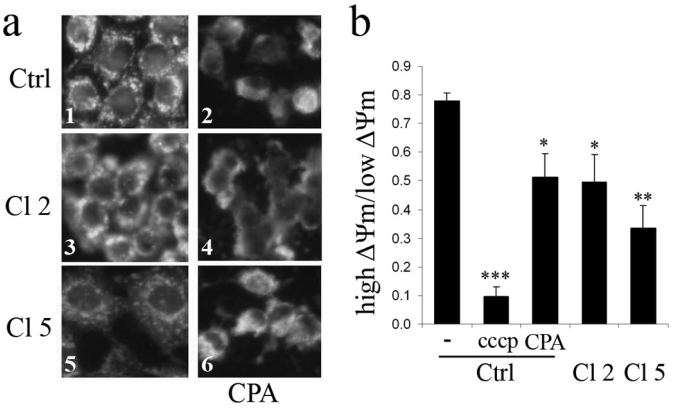

FIGURE 6. **Effect of PMCA2 overexpression on mitochondria morphology and membrane potential.** *a*, mitochondrial morphology. BRIN-BD11 cells (*Ctrl;* control) or cells transfected with PMCA2 (clones (*Cl*) 2 and 5) were treated (*panels 2*, *4*, and *6*) or not (*panels 1*, *3*, and *5*) for 24 h with CPA (50 μM) and stained with the mitochondrial marker Mitotracker green. Shown are representative images of four individual experiments. *b*, mitochondrial membrane potential. BRIN-BD11 cells (*Ctrl*) or PMCA2-overexpresing cells (clones 2 and 5) were treated or not (*Ctrl*) for 24 h with CPA or for 30 min with carbonyl cyanide *p*-chlorophenylhydrazone (CCCP). The $\Delta\Psi$m of the cell was determined by flow cytometry in cells stained with the DePsipher dye. Data are mean ± S.E. of four independent experiments expressed as a ratio of the two populations with either a high $\Delta\Psi$m or low $\Delta\Psi$m. *, $p < 0.05$; **, $p < 0.01$; and ***, $p < 0.001$ *versus* nontreated control.

As a second step, we examined mitochondrial function and morphology. Using the 3-(4,5-dimethylthiazol-2-yl)-2,5-diphenyl tetrazolium bromide assay to measure mitochondrial activity, we observed that under basal conditions, there was no difference between clone 5 and nontransfected cells (supplemental Fig. S4*b*), whereas mitochondrial activity of clone 2 was reduced by 40%. CPA and thapsigargin reduced mitochondrial activity in all cell preparations ($p < 0.001$; supplemental Fig. S4*b*). In control cells and clone 5, the effect of the SERCA inhibitors was modest (−15 to 20%), whereas in clone 2, the SERCA inhibitors more markedly reduced mitochondrial activity (−50%). Mitochondrial alteration was confirmed morphologically using the mitochondria-specific fluorescent probe Mitotracker Green (Fig. 6*a*). In control cells, the mitochondria displayed a punctated pattern with clear contours that disappeared in the presence of CPA, with the mitochondria now displaying a diffuse appearance. In the absence of CPA, mitochondria of clone 5 cells displayed a diffuse pattern, a phenomenon that was accentuated in clone 2. In the presence of CPA, a diffuse appearance similar to that seen in control cells was seen in clones 2 and 5 (Fig. 6*a*). Analysis by flow cytometry of live cells stained with DePsipher further revealed that PMCA2 overexpression or CPA treatment significantly reduced $\Delta\Psi$m as compared with untreated cells (Fig. 6*b* and Fig. supplemental Fig. S5). Carbonyl cyanide *p*-chlorophenylhydrazone (CCCP), a protonophore and uncoupler of oxidative phosphorylation, was used as a positive control. PMCA2-overexpressing cells displayed increased Bax translocation to the mitochondria and cytochrome *c* release (Fig. 7, *a* and *b* and supplemental Fig. S6). Quantitative assessment of the immunofluorescence experiments showed that under basal conditions, Bax translocation and cytochrome *c* release were increased in clone 2 and 5 compared with control cells. CPA increased both phenomenon but again to a larger extent in PMCA-overexpressing cells. Western blot analysis of antiapoptotic protein Bcl-2 and proapoptotic protein Bax revealed that in PMCA2-overexpressing cells, basal levels of Bax were increased ($p < 0.05$), whereas there was a tendency toward a decreased basal Bcl-2 expression (Fig. 7*c*). This resulted in a drastic increase in Bax/Bcl-2 ratio in PMCA2-overexpressing cells (Fig. 7*c*). CPA further increased this ratio, the effect being of larger magnitude in PMCA2-overexpressing than in control cells. During cell culture, clone 2 of PMCA2-overexpressing cells had a significantly longer doubling time than control cells ($p < 0.05$, supplemental Table S2).

DISCUSSION

In the present study, the combination of different aequorins and coelenterazines were used to determine the Ca^{2+} concentrations prevailing in the cytoplasm and mitochondria of insulin-secreting cells in response to K^+-induced membrane depolarization. Compared with fluorescent Ca^{2+} indicators, Ca^{2+}-bound aequorin has the advantage to be detected without illuminating the sample. Conversely, one disadvantage of aequorin is its irreversible consumption when exposed to a high [Ca^{2+}], a phenomenon that can be minimized or avoided by using aequorins recombined with coelenterazines both having different (lower) affinities for Ca^{2+}. The affinity of the complex for Ca^{2+} (and its consumption) also can be reduced by lowering the temperature from 37 to 22 °C (10). In the bulk of the cytoplasm, peak concentrations of 3–5 μM were observed. This is higher than the concentration measured in previous studies using fura-2 or aequorin (29–36). Fura-2 saturates at ~1 μM Ca^{2+}, but for aequorin, the reason of the discrepancy is unclear. The present values are in agreement with the concentrations required for exocytosis whether measured in permeabilized cells or in patch clamp experiments (37–40). Moreover, a concentration of ~35 μM was observed in a restricted zone of the cytoplasm, probably beneath the plasma membrane. This confirms the existence of Ca^{2+} heterogeneities in insulin-secreting cells (41–43; for a review, see Ref. 44). Of note, the concentration measured in the present study (30 μM) is the highest so far observed in an insulin-secreting cell and might correspond to the "microdomains" of high [Ca^{2+}] or high "Ca^{2+} hotspots" described in other tissues (9, 10). The existence of Ca^{2+} microdomains in pancreatic β-cells has been postulated based on theoretical grounds and on Ca^{2+} requirements for exocytosis. Although some authors found slightly higher Ca^{2+} levels beneath the plasma membrane or around secretory granules than in the bulk of the cytoplasm (33, 44), others using confocal spot detection methods (42) or fura-2 in cells stimulated by glucose or voltage-clamp depolarizations (38), respectively, measured Ca^{2+} concentrations ~7 μM near the plasma membrane. It was estimated that values up to 10 μM could be reached just beneath the plasma membrane, a value in the range of that found in the present study (35 μM).

In previous studies, higher Ca^{2+} concentration increases were observed in the mitochondria than in the cytosol, in response to various agents (34, 35, 45–47). However, the Ca^{2+} concentrations measured in the mitochondria in the present study were markedly higher than that measured in these previous studies. The reason for such a difference is that wild type

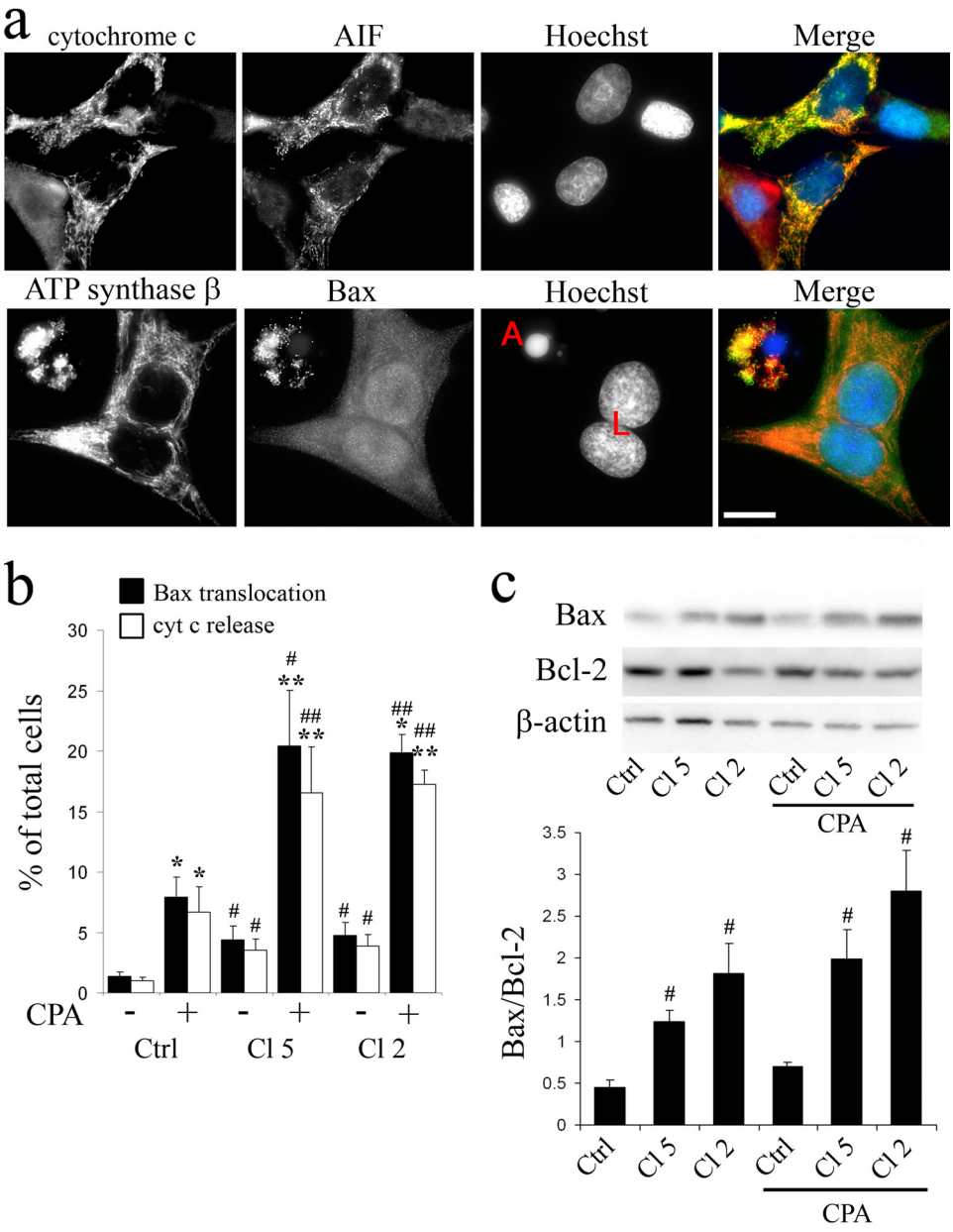

FIGURE 7. **Effect of PMCA2 overexpression on Bax/Bcl-2 ratio, Bax translocation, and cytochrome *c* release.** *a*, representative field showing live (*L*) and apoptotic cells (*A*) stained using anti-cytochrome *c*, anti-apoptosis-inducible factor (*AIF*), anti-ATP synthase β, anti-Bax antibodies, Hoechst, and a merged picture of all channels (*red*, cytochrome *c*; *green*, apoptosis-inducible factor; red, ATP synthase; *green*, Bax; *blue*, Hoechst). 100× magnification; the *scale bar* represents 10 μm. Apoptosis-inducible factor and ATP synthase β were used as mitochondrial markers. *b*, Bax translocation. Nontransfected BRIN-BD-11 cells (control; *Ctrl*) or cells transfected with PMCA2, clone 5 (*Cl 5*), and clone 2 (*Cl 2*), were treated or not for 24 h with CPA (50 μM). Bax translocation to the mitochondria and cytochrome *c* release from the mitochondria were evaluated by observation under a microscope after immunofluorescence using specific antibodies. The data are expressed as the percentage of cells showing Bax translocation and/or cytochrome *c* release over the total number of cells counted ± S.E. Results are means of four to five independent experiments. *, $p < 0.05$ and **, $p < 0.01$ *versus* respective nontreated control. #, $p < 0.01$ and ##, $p < 0.001$ *versus* respective nontransfected (control). *c*, nontransfected BRIN-BD-11 cells or cells transfected with PMCA2, clone 5, and clone 2 were treated or not for 24 h with CPA (50 μM). Bax and Bcl-2 expression were analyzed by Western blot. *Upper panel*, representative blot of Bax, Bcl-2, and β-actin. *Lower panel*, quantitative assessment of Bax over Bcl-2 levels. Results are means of four independent experiments. #, $p < 0.05$ *versus* respective non-transfected BRIN-BD11 (Ctrl).

aequorin and/or wild type coelenterazine were used in previous studies, whereas we used the mutated low Ca^{2+}-affinity aequorin and coelenterazine *n* that allow the measurement of higher Ca^{2+} concentrations. In a recent study, Quesada *et al.* (47) measured mitochondrial Ca^{2+} in digitonin permabilized islets using a low Ca^{2+} affinity aequorin set (low Ca^{2+} affinity-mutated mitochondrial aequorin and coelenterazine *n*) like in this study. Rises in medium $[Ca^{2+}]$ to 5 μM induced rapid increases in $[Ca^{2+}]_m$ up to 500 μM, in agreement with our observation. The finding of one single (initial) peak when mutated aequorin was recombined with coelenterazine *n* indicates subcellular heterogeneities in $[Ca^{2+}]$ among mitochondria, namely that the first peak reflects high Ca^{2+} increases in a limited number of mitochondria, probably localized close to the mouth of the voltage-sensitive Ca^{2+} channels. This also indicates that other mitochondria localized away from the region of high Ca^{2+}, display more modest increases in Ca^{2+}, as indicated by the small peaks on further stimulation of the cells using WT coelenterazine (Fig. 2*d*). Although our data are different from those of Rutter *et al.* (44) who failed to detect difference in Ca^{2+} increases in mitochondria located away or close to the plasma membrane, they are in agreement with data obtained in chromaffin cells where millimolar mitochondrial Ca^{2+} transients and a similar heterogeneity in mitochondrial Ca^{2+} responses are observed (10). Although the former data may appear to argue against the requirement of microdomains at the plasma membrane for rapid mitochondrial Ca^{2+} uptake during stimulated Ca^{2+} influx, they do not exclude such a view. Indeed, Quesada *et al.* (47) showed in digitonin-permabilized islets that Ca^{2+} uptake in mitochondria was observed at $[Ca^{2+}]_i$ as low as 500 nM, of course at a lower rate than at 5 μM.

In response to glucose, the cells displayed a succession of brief spikes both in the cytosol and the mitochondria in the micromolar (2 μM) or the tens of the micromolar (70 μM) range, respectively. This is at variance with a previous study, in aequorin-expressing INS-1 cells, in which a sustained increase in $[Ca^{2+}]_i$ and $[Ca^{2+}]_m$ were observed in response to glucose (35). The reason for this difference is unclear. In the case of the cytosolic response, the differences may due to difference in cell preparations or glucose concentrations used. It was mentioned under "Results" that some of the preparations showed an

increase in basal Ca^{2+} level on which spikes were superimposed. When using fura-2 to measure $[Ca^{2+}]_i$, BRIN cells stimulated by 11.1 mM glucose display large individualized Ca^{2+} spikes on an almost flat basal Ca^{2+} level (25). Primary β-cells behave in a similar way (29, 48). At the level of the mitochondria, the data cannot be compared with that of previous studies in view of the use of different aequorin/coelenterazine sets. Interestingly, however, the spikes induced by glucose in the cytosol, which were in the μM range (2 μM), generated spikes in the mitochondria that were in the tens of the micromolar range (70 μM). This confirms the view that the stimulation of our cells generates microdomains of high $[Ca^{2+}]$.

Our data show that PMCA overexpression reduces $[Ca^{2+}]_i$ and $[Ca^{2+}]_m$. The reduction was more pronounced in clone 2 than in clone 5, in good agreement with the higher PMCA expression in clone 2. Furthermore, the rate of apoptosis was higher in clone 2 than in clone 5, indicating that Ca^{2+} depletion in itself is instrumental. The Ca^{2+} depletion can be attributed to an increased Ca^{2+} extrusion from the cytoplasm. In a previous study, using fura-2 and furaptra, we showed that both the ER Ca^{2+} concentration and content were also reduced in PMCA-overexpressing cells (25).

To determine whether cell death was triggered via the ER or mitochondrial pathway, we studied the main UPR pathways (49). PMCA2 overexpression activated the IRE1α-XBP1s pathway as indicated by an increase in XBP1s expression under basal condition. In contrast, the PERK-eIF2α-CHOP and the ATF6-BiP pathways appeared to be inhibited in PMCA-overexpressing cells. Thus, there was a decrease in PERK and eIF2α phosphorylation together with a decrease CHOP mRNA response to SERCA inhibitors. Likewise, the two main chaperone systems in the ER (calnexin and calreticulin) and the heat shock protein BiP were decreased under basal and stressed conditions. Therefore, it is conceivable that chronic ER Ca^{2+} depletion hampers activation of the prosurvival UPR responses, sensitizing β-cells to ER stress-induced apoptosis. We have observed a similar pattern with INFγ treated β-cells, where an inhibition in the expression of β-cell chaperones sensitize these cells to CPA-induced apoptosis (50). From the data obtained, it is apparent that apoptosis was induced by Bax translocation and not from the activation of other proapototic pathways such as the PERK-eIF2α-CHOP pathway or from the activation of procaspase-12. Indeed, there was no change in caspase-12 expression and as above mentioned the PERK-eIF2α-CHOP pathway was inhibited. Bax contribution is suggested by (1) an increase in Bax expression together with (2) a tendency toward a decrease in Bcl-2 expression resulting in drastic increase in the Bax/Bcl-2 ratio, (3) an increase in Bax translocation from the cytosol to the mitochondria with subsequent cytochrome *c* release and (4) opening of the mitochondrial permeability transition pore with loss of mitochondrial membrane potential. In agreement with these data, PMCA overexpression altered mitochondrial function and morphology, the latter probably as a result of profound rearrangements of the submitochondrial structure (6).

Interestingly, $[Ca^{2+}]$ was not solely decreased in the cytoplasm and the ER of PMCA2-overexpressing cells but also in the mitochondria. In various models of cell death due to ER Ca^{2+} release and ER Ca^{2+} depletion, cell death is attributed to the uptake of Ca^{2+} by the mitochondria with resulting opening of the mitochondrial permeability transition pore and loss of the mitochondrial electrochemical gradient (1). Although the two latter changes were observed in our cells, they cannot be attributed to mitochondrial Ca^{2+} overload. ER Ca^{2+} depletion has been shown to have a biphasic effect on apoptosis, a reduced ER Ca^{2+} content exerting a protective effect, whereas a massive depletion increased the action of apoptotic agents (1). This suggests that PMCA overexpression induces a major Ca^{2+} depletion in our cells.

In conclusion, our study shows that insulin-secreting cell stimulation generates microdomains of high $[Ca^{2+}]_i$ and subcellular heterogeneities in $[Ca^{2+}]_m$ among mitochondria. PMCA overexpression depletes cytosolic, ER, and mitochondrial Ca^{2+} stores and induces apoptosis most probably through the mitochondrial pathway. If it is possible to increase the rate of apoptosis by PMCA overexpression, then it should be possible to obtain opposite effects by down-regulating the PMCA2 or the Na/Ca exchanger. Therefore, our data open the way to new strategies to control cellular Ca^{2+} homeostasis that could decrease β-cell apoptosis.

Acknowledgments—We thank A. Van Praet, M.-P. Berghmans, M. A. Neef, G. Vandenbroeck, M. Urbain, A. M. Musuaya, R. Makhnas, and S. Mertens for excellent technical support and Javier Garcia-Sancho (Instituto de Biologia y Genetica Molecular, Universidad de Valadolid, Valadolid, Spain) for help in setting up the aequorin luminometer.

REFERENCES

1. Orrenius, S., Zhivotovsky, B., and Nicotera, P. (2003) *Nat. Rev. Mol. Cell Biol.* **4,** 552–565
2. Mehmet, H. (2000) *Nature* **403,** 29–30
3. Nakagawa, T., Zhu, H., Morishima, N., Li, E., Xu, J., Yankner, B. A., and Yuan, J. (2000) *Nature* **403,** 98–103
4. Ron, D., and Walter, P. (2007) *Nat. Rev. Mol. Cell Biol.* **8,** 519–529
5. Zhang, K., and Kaufman, R. J. (2006) *Handb. Exp. Pharmacol.* **172,** 69–91
6. Kroemer, G., Galluzzi, L., and Brenner, C. (2007) *Physiol. Rev.* **87,** 99–163
7. Crompton, M., Barksby, E., Johnson, N., and Capano, M. (2002) *Biochimie* **84,** 143–152
8. Brenner, C., and Grimm, S. (2006) *Oncogene* **25,** 4744–4756
9. Rizzuto, R., and Pozzan, T. (2006) *Physiol. Rev.* **86,** 369–408
10. Montero, M., Alonso, M. T., Carnicero, E., Cuchillo-Ibáñez, I., Albillos, A., García, A. G., García-Sancho, J., and Alvarez, J. (2000) *Nat. Cell Biol.* **2,** 57–61
11. Pinton, P., and Rizzuto, R. (2006) *Cell Death Differ.* **13,** 1409–1418
12. Blaustein, M. P., and Lederer, W. J. (1999) *Physiol. Rev.* **79,** 763–854
13. Carafoli, E. (1994) *FASEB J.* **8,** 993–1002
14. Sokolow, S., Manto, M., Gailly, P., Molgó, J., Vandebrouck, C., Vanderwinden, J. M., Herchuelz, A., and Schurmans, S. (2004) *J. Clin. Invest.* **113,** 265–273
15. Bano, D., Young, K. W., Guerin, C. J., Lefeuvre, R., Rothwell, N. J., Naldini, L., Rizzuto, R., Carafoli, E., and Nicotera, P. (2005) *Cell* **120,** 275–285
16. Jeffs, G. J., Meloni, B. P., Sokolow, S., Herchuelz, A., Schurmans, S., and Knuckey, N. W. (2008) *Exp. Neurol.* **210,** 268–273
17. Molinaro, P., Cuomo, O., Pignataro, G., Boscia, F., Sirabella, R., Pannaccione, A., Secondo, A., Scorziello, A., Adornetto, A., Gala, R., Viggiano, D., Sokolow, S., Herchuelz, A., Schurmans, S., Di Renzo, G., and Annunziato, L. (2008) *J. Neurosci.* **28,** 1179–1184
18. Herchuelz, A., and Malaisse, W. J. (1981) *Diabetes Metab.* **7,** 283–288
19. Eizirik, D. L., and Mandrup-Poulsen, T. (2001) *Diabetologia* **44,**

2115–2133
20. Oyadomari, S., Takeda, K., Takiguchi, M., Gotoh, T., Matsumoto, M., Wada, I., Akira, S., Araki, E., and Mori, M. (2001) *Proc. Natl. Acad. Sci. U.S.A.* **98,** 10845–10850
21. Cardozo, A. K., Ortis, F., Storling, J., Feng, Y. M., Rasschaert, J., Tonnesen, M., Van Eylen, F., Mandrup-Poulsen, T., Herchuelz, A., and Eizirik, D. L. (2005) *Diabetes* **54,** 452–461
22. Diaz-Horta, O., Kamagate, A., Herchuelz, A., and Van Eylen, F. (2002) *Diabetes* **51,** 1815–1824
23. Brini, M. (2008) *Methods* **46,** 160–166
24. McClenaghan, N. H., Barnett, C. R., Ah-Sing, E., Abdel-Wahab, Y. H., O'Harte, F. P., Yoon, T. W., Swanston-Flatt, S. K., and Flatt, P. R. (1996) *Diabetes* **45,** 1132–1140
25. Kamagate, A., Herchuelz, A., and Van Eylen, F. (2002) *Diabetes* **51,** 2773–2788
26. Brini, M., Marsault, R., Bastianutto, C., Pozzan, T., and Rizzuto, R. (1994) *Cell Calcium* **16,** 259–268
27. Brini, M., Marsault, R., Bastianutto, C., Alvarez, J., Pozzan, T., and Rizzuto, R. (1995) *J. Biol. Chem.* **270,** 9896–9903
28. Salvioli, S., Ardizzoni, A., Franceschi, C., and Cossarizza, A. (1997) *FEBS Lett.* **411,** 77–82
29. Herchuelz, A., Pochet, R., Pastiels, C., and Van Praet, A. (1991) *Cell Calcium* **12,** 577–586
30. Grapengiesser, E., Gylfe, E., and Hellman, B. (1988) *Biochem. Biophys. Res. Comm.* **151,** 1299–1304
31. Wang, J. L., and McDaniel, M. L. (1990) *Biochem. Biophys. Res. Commun.* **166,** 813–818
32. Pralong, W. F., Bartley, C., and Wollheim, C. B. (1990) *EMBO J.* **9,** 53–60
33. Theler, J. M., Mollard, P., Guérineau, N., Vacher, P., Pralong, W. F., Schlegel, W., and Wollheim, C. B. (1992) *J. Biol. Chem.* **267,** 18110–18117
34. Rutter, G. A., Theler, J. M., Murgia, M., Wollheim, C. B., Pozzan, T., and Rizzuto, R. (1993) *J. Biol. Chem.* **268,** 22385–22390
35. Kennedy, E. D., Rizzuto, R., Theler, J. M., Pralong, W. F., Bastianutto, C., Pozzan, T., and Wollheim, C. B. (1996) *J. Clin. Invest.* **98,** 2524–2538
36. Van Eylen, F., Lebeau, C., Albuquerque-Silva, J., and Herchuelz, A. (1998) *Diabetes* **47,** 1873–1880
37. Wollheim, C. B., Ullrich, S., Meda, P., and Vallar, L. (1987) *Biosci. Rep.* **7,** 443–454
38. Bokvist, K., Eliasson, L., Ammälä, C., Renström, E., and Rorsman, P. (1995) *EMBO J.* **14,** 50–57
39. Takahashi, N., Kadowaki, T., Yazaki, Y., Miyashita, Y., and Kasai, H. (1997) *J. Cell Biol.* **138,** 55–64
40. Barg, S., Ma, X., Eliasson, L., Galvanovskis, J., Göpel, S. O., Obermüller, S., Platzer, J., Renström, E., Trus, M., Atlas, D., Striessnig, J., and Rorsman, P. (2001) *Biophys. J.* **81,** 3308–3323
41. Gylfe, E., Grapengiesser, E., and Hellman, B. (1991) *Cell Calcium* **12,** 229–240
42. Quesada, I., Martín, F., and Soria, B. (2000) *J. Physiol.* **525,** 159–167
43. Pinton, P., Tsuboi, T., Ainscow, E. K., Pozzan, T., Rizzuto, R., and Rutter, G. A. (2002) *J. Biol. Chem.* **277,** 37702–37710
44. Rutter, G. A., Tsuboi, T., and Ravier, M. A. (2006) *Cell Calcium* **40,** 539–551
45. Maechler, P., Kennedy, E. D., Pozzan, T., and Wollheim, C. B. (1997) *EMBO J.* **16,** 3833–3841
46. Nakazaki, M., Ishihara, H., Kakei, M., Inukai, K., Asano, T., Miyazaki, J. I., Tanaka, H., Kikuchi, M., Yada, T., and Oka, Y. (1998) *Diabetologia* **41,** 279–286
47. Quesada, I., Villalobos, C., Núñez, L., Chamero, P., Alonso, M. T., Nadal, A., and García-Sancho, J. (2008) *Cell Calcium* **43,** 39–47
48. Tengholm, A., and Gylfe, E. (2009) *Mol. Cell. Endocrinol.* **297,** 58–72
49. Eizirik, D. L., Cardozo, A. K., and Cnop, M. (2008) *Endocr. Rev.* **29,** 42–61
50. Pirot, P., Eizirik, D. L., and Cardozo, A. K. (2006) *Diabetologia* **49,** 1229–1236